Transition between N- and Z-shaped current-voltage characteristics in semiconductor multiple-quantum-well structures

O. V. Pupysheva[a)]
Institute for Materials Research, Tohoku University, Sendai 980-8577, Japan
and Department of Low Temperature Physics, Faculty of Physics,
M. V. Lomonosov Moscow State University, Moscow 119992, Russia

A. V. Dmitriev
Department of Low Temperature Physics, Faculty of Physics, M. V. Lomonosov Moscow State University, Moscow 119992, Russia

A. A. Farajian, H. Mizuseki, and Y. Kawazoe
Institute for Materials Research, Tohoku University, Sendai 980-8577, Japan

(Received 17 January 2006; accepted 17 June 2006; published online 14 August 2006)

We study theoretically the vertical electron transport in semiconductor multiple-quantum-well structures, where sequential tunneling between neighboring wells takes place. The nonuniformity of electric field along the growth axis and charge redistribution among the quantum wells, as well as between the inner wells and contacts, are taken into account. A simple and efficient model of charged contact layers is proposed. The calculated *I-V* curves exhibit regions of conventional N-shaped negative differential conductivity and Z-shaped portions of intrinsic bistability, both arising due to the tunneling resonances. A general explanation of their formation mechanism is given, which is valid for any form of interwell transitions of resonant nature. The conditions of N- and Z-shaped curve observation and controllable transition between them are discussed. © *2006 American Institute of Physics*. [DOI: 10.1063/1.2234546]

I. INTRODUCTION

The most interesting and important feature of semiconductor superlattices (SLs) and multiple-quantum-well (MQW) structures is that their current-voltage (*I-V*) characteristics usually possess a region of negative differential conductivity (NDC). It arises due to the tunneling resonances between different quantum wells. In the structures with low-transparent quantum barriers separating the wells, the formation of NDC regions is associated with nonuniformity of the electric field in the vertical direction (along the growth axis). The formation of high-field domains in superlattices was considered as early as 30 years ago by Esaki and Chang.[1] The feedback mechanism linking the changes in potential energy with carrier trapping in the quantum well was discussed by Ricco and Azbel.[2] This leads to a necessity to solve the problem of mathematical description of the vertical electron transport in MQW structures self-consistently.

Within the last 20 years, double-barrier resonant-tunneling structures (DBRTSs) were intensively studied, both experimentally and theoretically. Bistability of their *I-V* characteristics, i.e., existence of two current values corresponding to the same voltage due to a resonance between the cathode (emitter) and the quantum well, was found experimentally by Goldman *et al.*[3] It's intrinsic character was proposed and clarified in further discussion.[4] The authors explained the obtained results using the sequential tunneling approach and taking into account charge accumulation in the quantum well, in agreement with the observed system behavior in magnetic field.[5]

These experiments immediately gave rise to numerous theoretical investigations of DBRTSs (see, e.g., Refs. 6 and 7). In particular, it was noticed[7] that they may actually exhibit not bi- but tristability; however, the term bistability remains more common in the literature. The negative output resistance technique, proposed later,[8,9] made it possible to directly observe continuous Z-shaped *I-V* curves of semiconductor double-barrier structures instead of conventional N-shaped ones.

The problem of current instability and dynamical behavior arises here, as in every system manifesting a multistable *I-V* characteristic and/or NDC.[10] Stability of the central branch of the Z-shaped region was studied in Refs. 11 and 12 within the sequential tunneling model. The general features of the current density front propagation in the systems with Z-shaped current-voltage curves are compared with those of more familiar *S*-type systems, for example, by Meixner *et al.*[13] Interesting details regarding the lateral transport and lateral current density fronts in DBRTSs can be found, e.g., in Refs. 14 and 15. However, in the discussion below we assume no inhomogeneity along the layers of the structure and discuss only vertical charge transport.

Behavior of relatively long SL and MQW structures under electric field is similar to that of DBRTSs. The contemporary situation and the latest achievements in the study of vertical electron transport in semiconductor SL can be found in recent comprehensive reviews.[16,17]

Time-independent models, reasonably describing multistable SL with electric field domains, were proposed by Bonilla *et al.*[18] and Prengel *et al.*[19] They used a combination of the rate equations, within the framework of the sequential

[a)]Electronic mail: olga.pupysheva@rice.edu

tunneling approach, and the discrete Poisson equation. There have been many subsequent works modeling the sequential tunneling transport, in particular, time dependent, in weakly coupled semiconductor SLs.[20–31] However, they use some specific assumptions, which make it difficult to generalize the obtained results. This concerns, first of all, the particular form of electric field dependence of the transition probabilities between the electron states localized in different quantum wells, or, alternatively, the electron drift velocity. In particular, the probability of reverse transition is often taken to be zero, while sometimes it is not negligible.

As concerns the most commonly used boundary conditions, the electron concentrations n_1 and n_N in anode and cathode are either taken equal to the concentrations in the adjacent inner wells of the superlattice ($n_1=n_2$, $n_N=n_{N-1}$)[19–22] or fixed at some constant levels (not necessarily equal to each other).[22–24] In the former model there is no electric field in the leftmost and rightmost quantum barriers of SL, while the latter does not account for the dependence of n_1 and n_N on the applied voltage and current density values. Both of these assumptions can be improved.

Interestingly, the same problem was properly solved for DBRTS long ago,[5] by applying the condition of electrical neutrality of the whole system including the accumulation and depletion layers of cathode and anode, respectively. But in studies of SL the global charge conservation[26–29] or similar boundary conditions[30] were utilized in only a few papers, and only one among them was devoted to the stationary transport.[26] However, the *I-V* curves calculated in Ref. 26 contain few self-crossings, which is unusual and might be due to the approximations used in this work for the transition probabilities corresponding to the leftmost and rightmost quantum barriers. The current status of the contact modeling problem is discussed in detail in the reviews.[16,17]

In the present work we develop a rather general model for calculations of the stationary electron transport in MQW structures, with simple and efficient description of the contact effects. We do not consider dynamical phenomena, such as movement of the high-field domains and current oscillations, and restrict ourselves to the steady state. Solving the Poisson and kinetic equations self-consistently provides us with nonlinear electric field and carrier distribution in the MQW structure. We include the carrier concentrations in the contacts as variables to be calculated and use the global charge conservation for the whole system. We also take into account the continuity of the energy spectra of the contacts.

This work gives a clear explanation of the occurrence of the N- and Z-shaped *I-V* curves. This explanation is independent of the particular form of the transition probabilities between the neighboring wells, as long as the transitions are of resonant nature. Unlike many other works, we do not neglect the reverse electron transitions between the quantum wells. Furthermore, the current-voltage characteristics of the structures with different numbers of quantum wells are compared. We derive the conditions of the transition between N- and Z-shaped curves with increase of the number of layers. This provides a possibility to control the appearance or disappearance of intrinsic bistability in MQW structures.

Let us mention that our model does not use the periodicity of the MQW structure, and thus is applicable for the transport study in disordered systems.[32] Although we consider only periodic structures in the present work, the discussed mechanism of the transition between N- and Z-shaped *I-V* curves is quite general and holds for disordered structures as well.

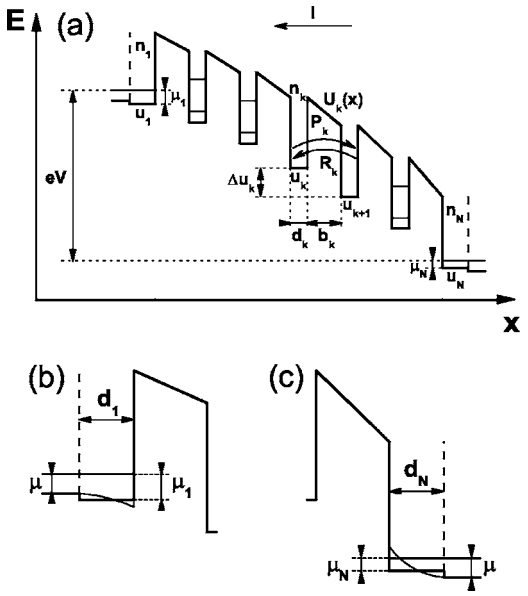

FIG. 1. Schematic model of the potential profile of MQW structure under electric field (a), cathode (b), and anode (c).

II. MODEL

The model of the potential profile of *n*-type MQW structure under electric field is schematically shown in Fig. 1(a). We consider a structure with thick quantum barriers of widths b_k, much larger than well widths d_k. Consequently, the potential variations in the quantum wells can be neglected, and the well potentials u_k are taken to be constant. We assume for simplicity that only the wells are doped; the two-dimensional (2D) concentrations of electrons and donors in the kth quantum well are n_k and n_k^0, respectively. As for the quantum barriers, they are supposed to bear no electric charge, and thus the electric field in them is constant, and the potentials $U_k=U_k(x)$ depend linearly on the coordinate along the growth axis. The low-transparent barriers allow us to consider the electron states as localized in the quantum wells and the vertical transport as sequential electron tunneling between the states localized in adjacent wells.

We not only consider the charge redistribution among the inner quantum wells but also account for the electrodes (cathode and anode), and, in particular, for charge accumulation and depletion layers in them. Following Refs. 19 and 24, we describe the contact layers as two additional, first and Nth, quantum wells of fixed widths d_1 and d_N, respectively. The total number N of wells in the structure includes N_w inner quantum wells and two contact layers. Notice that the energy spectra in the contact layers are continuous and the 2D electron concentrations n_1 and n_N enter our equations as unknown variables to be calculated. This distinguishes our model from those of Refs. 19 and 24.

The electron concentrations in the electrodes outside the charged areas are uniform and do not vary. We assume that there is no electric field in these outer, electrically neutral parts of the electrodes. The band bending effect in the charge accumulation and depletion layers, shown by thin solid lines in Figs. 1(b) and 1(c), is effectively included in our model. Namely, a step function is substituted for the actual space-variable potential in the contact layers. This function takes the values u_1 and u_N in cathode and anode, respectively. We assume that for any contact charge value, the electron chemical potential in the contact layer coincides with the chemical potential in the outer part of the same electrode, see Figs. 1(b) and 1(c). Correspondingly, the voltage drop across the MQW structure under consideration is given by the equality

$$V = \frac{u_1 + \mu_1 - u_N - \mu_N}{e} = \frac{1}{e}\sum_{k=1}^{N-1} \Delta u_k + \frac{\mu_1 - \mu_N}{e}. \tag{1}$$

Here $\Delta u_k = u_k - u_{k+1}$ is the potential drop across the kth quantum barrier, and μ_1 and μ_N, the chemical potentials in the charged layers of contacts, are functions of electron concentrations n_1 and n_N and temperature, as follows from the Fermi statistics.

This contact description is consistent with the assumption of rectangular shape of the inner quantum wells used in the present work and works well when the accumulation and depletion layers are thin. This is true in the case of heavily doped contacts, which we adopt here. Our model accounts for the most important features of the system, its electrical neutrality and a connection between the electrical charge in contacts and bias applied to the structure. At the same time it has the advantages of being simple and efficient for calculations, as compared with the more sophisticated models of contacts.[5,26,30] These properties are especially important when a complicated structure with numerous layers is to be considered, as in the present work.

Let us now discuss the equations we use to describe the vertical electron transport in MQW structure.

The charge of the kth quantum well is connected with the electric field in the surrounding barriers by integrating the Poisson equation:

$$n_k^0 - n_k = \frac{1}{4\pi e}(D_k - D_{k-1}), \tag{2}$$

where e is the absolute value of the electron charge. The induction D_k of the electric field in the kth barrier determines the relative potential shift of the neighboring quantum wells, according to the formula

$$D_k = \frac{\varepsilon}{e}\frac{(u_{k+1} - u_k - u_{k+1}^0 + u_k^0)}{b_k}. \tag{3}$$

Here u_k^0 and u_{k+1}^0 are the values of the well potentials in the absence of the electric field and without charge redistribution in the structure, when all the wells are electrically neutral.

As discussed above, there is no electric field to the left of the cathode accumulation layer and to the right of the anode depletion layer (see Fig. 1). This means that the whole MQW structure including the charged contact layers stays electrically neutral:

$$\sum_{k=1}^{N} (n_k - n_k^0) = 0. \tag{4}$$

With this assumption, the equalities similar to Eq. (2) are valid for both the contact layers ($k=1,N$), with $D_0 = D_N = 0$. As there are no quantum wells in the outer parts of the electrodes, u_0 and u_{N+1} values are not defined in our model. In order to write the formal expressions analogous to Eq. (3) for D_0 and D_N, we set $u_0 = u_1$, $u_0^0 = u_1^0$, and $u_{N+1} = u_N$, $u_{N+1}^0 = u_N^0$.

The kinetic equation for the current density between any two adjacent wells, or a well and a contact, under dc conditions can be expressed via P_k and R_k, the integral probabilities per unit time of the direct and reverse electron transitions:

$$I = e(P_k n_k - R_k n_{k+1}). \tag{5}$$

The transition probabilities depend on many factors, the most important being electron momentum distribution in the wells, energy spectra, and physical mechanism of interwell transitions.

We assume that the carrier distribution is classical in the inner wells but may be degenerate in heavily doped contacts; so the distribution is described by the temperature and (in contacts only) by the Fermi energy.

In our model the electric field does not influence the size-quantization energies in the wells, so that the electron states in each well shift together with the conduction band bottom on the energy scale. Hence the probabilities depend on the field only through Δu_k, the potential shift of the energy levels in the adjacent wells.

As concerns the interwell transitions, they can be accompanied by acoustical-phonon, optical-phonon, or impurity scattering. The choice of the structure material, temperature, and the layer parameters, presented in Appendix A, allows us to simplify the model by neglecting the electron-phonon interaction. The applicability of this approach, which is similar to the one used in Ref. 32, is discussed in Appendix B. Therefore, in the current work we consider an important mechanism of the electron interaction with charged donors in the quantum wells, although a generalization for any scattering mechanism is also possible.

As the Coulomb matrix element is proportional to $[(\Delta\mathbf{p})^2 + (\hbar/r_D)^2]^{-1/2}$, where $\Delta\mathbf{p}$ is the electron momentum change accompanying the transition and r_D is the Debye screening radius, the corresponding probability reaches a maximum when the interwell transition with zero $\Delta\mathbf{p}$ is possible. The ionized impurity assisted transition is elastic, so this takes place when the energy levels in the neighboring wells coincide. In contrast, when an energy shift between the wells appears, a change of the in-plane momentum must accompany the transition, and hence the transition probability decreases (see details in Appendix B).

As a consequence, the probabilities P_k and R_k have a resonant form, i.e., they have maxima for such u_k and u_{k+1} values when the energy levels in the neighboring wells coincide, that is, when they are in resonance. The transition probabilities used in our work are depicted in Fig. 2 as functions of Δu_k for the structure parameters presented in Appendix A.

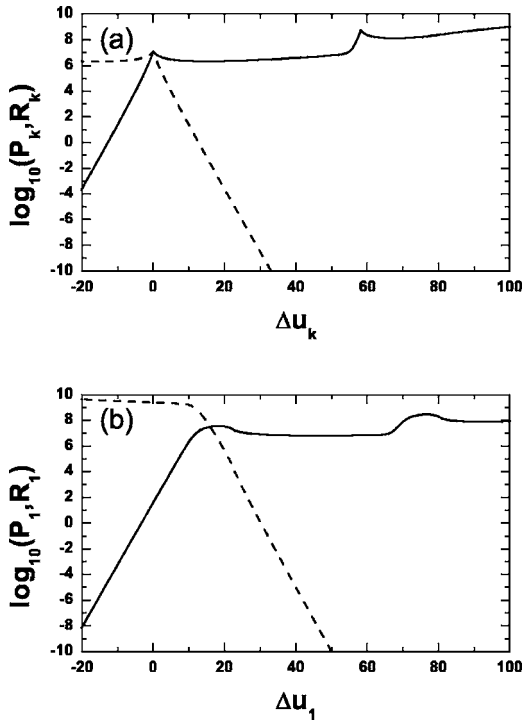

FIG. 2. Decimal logarithm of direct (solid line) and reverse (dashed line) transition probabilities (in 1/s) of Appendix B vs potential drop (in meV) in the corresponding quantum barrier: transitions between two equivalent inner quantum wells (a) and transitions between the cathode and the adjacent inner well (b). The structure parameters are described in Appendix A. Two maxima of the direct transition probabilities P_k are observed for $\Delta u_k \geqslant 0$, because there are two size-quantization levels in each quantum well, which can coincide either with the states localized in the neighboring wells or with the Fermi energy in cathode.

Let us stress that the formation mechanism of the observed *I-V* curve peculiarities to be explained below is valid for any form of the transition probabilities as functions of Δu_k as long as they keep a resonant shape. So our explanation is rather general, which is its important advantage.

III. RESULTS AND DISCUSSION

The system of equations (2)–(5) can be rewritten as follows:

$$n_k = n_k^0 + \frac{\varepsilon}{4\pi e^2}\left(\frac{\Delta u_k - \Delta u_k^0}{b_k} - \frac{\Delta u_{k-1} - \Delta u_{k-1}^0}{b_{k-1}}\right), \tag{6}$$

$$I = eP_k n_k - eR_k n_{k+1}, \tag{7}$$

$$\sum_{k=1}^{N} n_k = \sum_{k=1}^{N} n_k^0 = \text{const}, \tag{8}$$

$$\Delta u_0 = \Delta u_0^0 = \Delta u_N = \Delta u_N^0 = 0.$$

This nonlinear system consists of $(2N-1)$ equations in $(2N-1)$ variables Δu_k and n_k. For the *n*-type MQW structures studied here, the physically meaningful solutions are those with positive electron concentrations n_k. As can be easily seen from the kinetic equation (7), the condition $n_N > 0$ ensures $n_k > 0$ for all k. Therefore, the donor concentration in the anode depletion layer should be taken large enough to provide the desired voltage value, in analogy to a plane capacitor.

The system of equations (6)–(8) is solved self-consistently for a given current value in the following way. For arbitrary electron concentration n_k and potential drop Δu_k, one can easily obtain Δu_{k-1} and then n_{k-1}, successively using Eqs. (6) and (7). After repeating this procedure for $k = N, \ldots, 2$, that is, from anode to cathode, all the unknown variables are expressed through n_N. To close the system, the global charge conservation, Eq. (8), is solved numerically. All the possible n_N values are found by means of shooting algorithm, and then for each n_N concentration the other unknown variables are determined, including parameters of the two contacts and the total voltage drop across the MQW structure.

Let us mention that if one repeats the procedure described above in the opposite direction, i.e., from cathode to anode, the accuracy of the numerical solution will decrease significantly. The reason is that, when finding the concentration n_{k+1} from Eq. (7), one needs to divide a small value $(eP_k n_k - I)$ by another small value, eR_k. Furthermore, the electron concentration in cathode n_1 is larger than all the other electron concentrations, and a small relative change in its value would result in larger relative changes in all n_k.

The numerically calculated *I-V* curves of double- and multiple-quantum-well structures exhibit both Z- and N-shaped regions, as one can see from Fig. 3. Each of current maxima is observed when the energy states in a pair of neighboring wells are in resonance. It is worth mentioning that the form of the Z-shaped regions in Fig. 3 is quite similar to those obtained experimentally.[8,9]

There are two different types of these current maxima, those corresponding to the resonances in a pair of the adjacent inner quantum wells and those caused by the resonances between the cathode and the second well. The former type is related to the maximum of the transition probability $P_k(\Delta u_k)$ for $k > 1$ [shown in Fig. 2(a)], while the latter is realized in the vicinity of a $P_1(\Delta u_1)$ maximum [depicted in Fig. 2(b)]. Due to the nonlinearity of the electric field distribution along the growth axis of the structure, the Δu_k values increase with k (see, e.g., stationary electric field profiles in Refs. 19–21 and 23–26). As a result, for larger k, the resonance between kth and $(k+1)$th wells and the corresponding current maximum are shifted to a lower voltage. So, for any of the curves in Fig. 3 the current maximum observed at the lowest voltage corresponds to the resonance between the rightmost inner quantum well and the previous one, i.e., to the maximum of $P_{N-2}(\Delta u_{N-2})$ transition probability; the next current maximum corresponds to the resonance between $(N-2)$th and $(N-3)$th wells, etc. The last two current maxima at higher voltages correspond to the $P_1(\Delta u_1)$ transition probability maxima, occurring when the Fermi level in cathode is close to one of the two size-quantization levels in the adjacent inner well (see Fig. 2 and its caption).

The number of maxima on the *I-V* curve increases for the longer structures, i.e., for those with larger N. Namely, for the structures under consideration, which have two energy levels in each quantum well, one can expect totally $(N-1)$ current maxima. (N_w-1) of them correspond to the

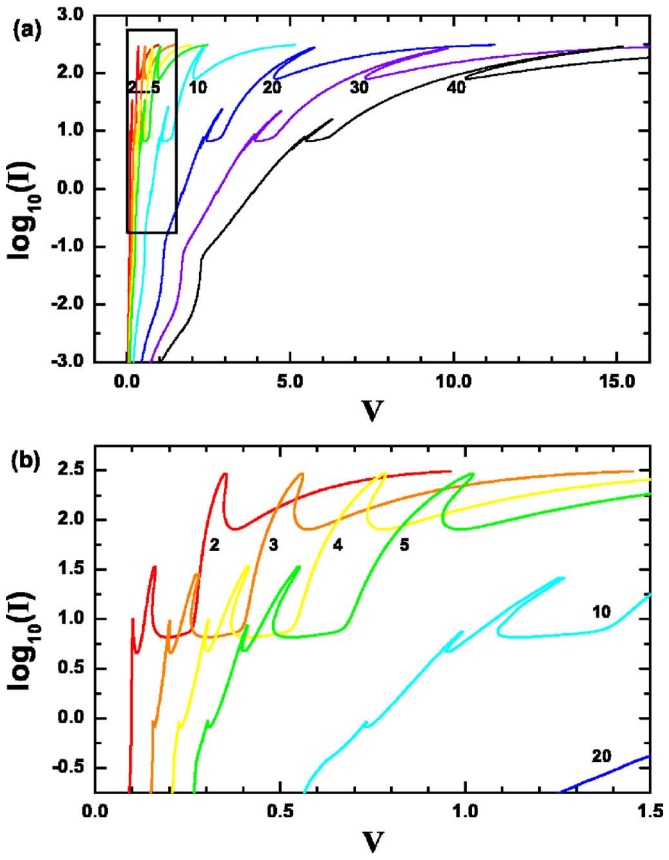

FIG. 3. (Color online) Decimal logarithm of current density (in A/cm^2) vs voltage (in V) for the MQW structures with different numbers of layers. Each curve is labeled by the numbers of inner quantum wells $N_w=N-2$. The structure parameters and transition probabilities are given in Appendixes A and B. Boxed part of upper panel (a) is zoomed in a lower panel (b).

resonances between the inner wells, and the last two are caused by the resonances between the cathode and the adjacent inner well, as discussed above. However, due to the low barrier transparence, some minor maxima in the low-field region cannot be clearly distinguished against the background of the fast growth of the curves (see Fig. 3). Moreover, if all the quantum barriers in the structure have the same width and height, then the probabilities of transitions through the leftmost and rightmost barriers, calculated as described in Appendix B, turn out to be much lower than all the others. This happens because of the relatively small number of electrons at the Fermi level of the corresponding contact, due to its continuous energy spectrum. In this case only two current maxima, which correspond to the maxima of $P_1(\Delta u_1)$, can be observed for any N. To make the other current maxima visible, one has to take the first and last barriers thinner than those inside the MQW structure, as it is done in the present work (see structure parameters in Appendix A).

Let us now compare the I-V curves for any pair of MQW structures with different numbers of quantum wells, N_1 and (N_1+N_2). As can be seen from Fig. 3, the maximum current densities, which are reached at the resonance in the same pair of adjacent wells, are almost equal in short and long structures. They are determined by the maximum, resonant values of the corresponding transition probability P_k. The corresponding voltages, however, significantly increase with N.

To explain this, we can roughly describe the longer MQW structure as a series connection of two shorter ones, containing N_1 and N_2 wells.[33] It is very unlikely that two resonances could take place simultaneously in both of these parts of the long structure, because the electric field distribution along the growth axis is inhomogeneous. Therefore, when considering a resonance in the first part containing N_1 wells, we can model the second part as having a regular, monotonously increasing I-V curve.

Let the current I correspond to the voltages V_1 in the first short structure and V_2 in the second one, taking into account the actual electron redistribution in each of them.[33] Then the same current value would be observed at the voltage (V_1+V_2) in the whole long structure. As a result, the shift of I-V curve along the voltage axis for the long structure, as compared with the short one, equals V_2. Thus, the higher the current density, the higher is the V_2 value, and hence the stronger the I-V curve deformation becomes for the long structure. In particular, this leads to a transition from conventional N-shaped current maxima to Z-shaped ones and to the elongation of the voltage interval where Z-shaped regions of the curve are observed. A similar transformation of I-V curves can be observed as a result of an increase of the doping level in the quantum wells.[24,25] Our results are in agreement with those of a different model by Wacker *et al.*[25]

It is worth noting that the mechanism of such Z-shaped peculiarity is intrinsic. It should not be confused with an extrinsic bistability,[3,4] which might arise from the series resistance of the Ohmic contacts[34] or other external resistors.[35,36] The intrinsic bistability discussed here originates from the behavior of various internal parts of the structure under consideration. It is based on the electrostatic feedback including the charge redistribution and accumulation in the quantum wells, similar to the mechanism proposed in Ref. 3 for DBRTS.

The peculiarities of I-V curves can be also described analytically from a different point of view, using the following simplifying approximation. The electron current in the reverse direction (from right to left in Fig. 1) quite often can be neglected as compared to the direct current: $R_k n_{k+1} \ll P_k n_k$. Then the kinetic equation can be rewritten in the form

$$I \approx e P_k n_k. \tag{9}$$

Here the probability P_k is a function of Δu_k and of the chemical potentials in the case of the degenerate electron distribution (for $k=1$ and $N-1$), as discussed earlier. As concerns the electron concentration, $n_k=n_k(\Delta u_k, \Delta u_{k-1})$, according to Eq. (6). This allows us to recursively calculate the derivatives of all the variables in terms of the single potential drop Δu_j for some particular j. An extremum of I-V curve takes place when

$$\frac{dI}{dV} = \frac{dI/d(\Delta u_j)}{dV/d(\Delta u_j)} = 0, \tag{10}$$

that is, when either

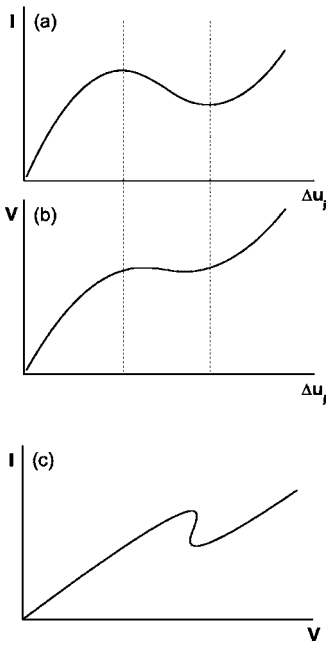

FIG. 4. Sample characteristics of current density vs electric field in the jth quantum barrier (a), voltage drop across the whole MQW structure vs electric field in the jth quantum barrier (b), and current density vs voltage drop across the whole MQW structure, possessing a Z-shaped region (c).

$$\frac{dI}{d(\Delta u_j)} = 0 \tag{11}$$

or

$$\frac{dV}{d(\Delta u_j)} = \infty. \tag{12}$$

As can be seen from Eq. (9), equality (11) can be fulfilled in the vicinity of an extremum of $P_j(\Delta u_j)$, i.e., when a resonance occurs between the jth and $(j+1)$th quantum wells. As shown schematically in Fig. 4, with the increase of Δu_j, the differential conductivity of the jth quantum barrier changes its sign and becomes negative. At the same time, for all the other, nonresonant barriers in the rest of the structure it remains positive. Thus, the voltage across the rest of the structure decreases as the current decreases. Together with the growing voltage across the jth barrier, this may lead either to an increase or to a decrease of the bias applied to the whole structure, according to Eq. (1). In the former case a conventional N-shaped region of the I-V curve is formed, while the latter corresponds to a Z-shaped region, depicted in Fig. 4.

Condition (12) is fulfilled when at least one of the functions $\Delta u_k(\Delta u_j)$, entering the sum in Eq. (1), has an infinite derivative. Then $d(\Delta u_j)/d(\Delta u_k)=0$, which can happen when the resonance occurs between the kth and $(k+1)$th wells. The behavior of the functions $I(\Delta u_k)$ and $V(\Delta u_k)$ is analogous to those discussed in the previous paragraph, and the corresponding region of the I-V characteristic, again, can have either N-like or Z-like form.

The electron concentration n_j rises with the increase of Δu_j and decrease of Δu_{j-1}, according to Eq. (6). If n_j increases with Δu_j while P_j decreases, their product, which gives the current density by Eq. (9), might grow monotonously. Then none of conditions (11) and (12) is fulfilled. This means that for a very smooth $P_j(\Delta u_j)$ maximum the corresponding part of the I-V curve may have no maximum. Such situation is realized when the jth barrier has relatively high transparence. Then the resonance between the jth and $(j+1)$th quantum wells would not affect much the system behavior.

One can see from this explanation that the quantities which control the occurrence of N- and Z-shaped portions of I-V curves are the two derivatives in the nominator and denominator of Eq. (10). These derivatives are determined by the sharpness of the maximum of the transition probability functions $P_j(\Delta u_j)$ and by the effective differential conductivity of the nonresonant part of the structure, correspondingly. In particular, a faster decrease of the transition probability with the potential drop Δu_j in the resonant part of the structure results in a faster decrease of the current density I and of the voltage across the nonresonant part of the structure. Then the formation of Z-shaped current maxima is more favorable than for a smoother $P_j(\Delta u_j)$ peak.

Now it is clear that to observe both conventional NDC and intrinsic bistability, as well as transitions between them, the structures with relatively thick quantum barriers should be taken. One could already notice that the barrier widths in the MQW structures under consideration are taken larger than in many other works, where relatively thin, although still low-transparent, quantum barriers are studied. As a side effect, this decreases the current density values obtained in the present work in comparison with those of the other works, and shifts the current maxima away from each other. Decreasing the transparence of the MQW structure, one can easily cause the transitions between N- and Z-shaped current-voltage characteristics. This can be achieved by increasing either the width, or the height, or the number of quantum barriers, the latter case being demonstrated in Fig. 3.

Let us emphasize that the explanation given above is valid for any functions $P_k(\Delta u_k)$ and $R_k(\Delta u_k)$ of resonant nature. For example, one can consider a MQW structure with both ionized impurity and optical-phonon scattering. This would lead to the formation of the P_k and R_k peaks for such Δu_k values when the size-quantization levels in the neighboring wells either have the same energies or are separated by $\hbar\omega_{\mathrm{LO}}$. Importantly, the corresponding current maxima of the I-V curve would have N- or Z-like shape, still determined by the factors discussed in the present work.

Moreover, transitions from N- to Z-shaped I-V curves might take place not only in the semiconductor MQW structures but also in other quasi-one-dimensional systems with NDC, for example, in carbon nanotubes.[37,38] Intrinsic bistability can be observed in such systems due to the defects or doping, decreasing the differential conductivity of their nonresonant parts. The transition mechanism discussed here does not depend on the origin of the negative differential conductivity.

IV. CONCLUSIONS

We studied vertical electron transport in semiconductor multiple-quantum-well structures within the sequential tun-

neling approach and under assumption of resonant interwell transitions. The Poisson equation and kinetic equation for the current were solved self-consistently for the electrostatic potentials of the wells and electron concentrations in them. A simple and efficient model of contacts was proposed. The calculated dc *I-V* curves exhibit conventional N-shaped NDC regions as well as Z-shaped regions of intrinsic bistability, both arising due to the tunneling resonances. A general explanation of their origin was given, valid for any form of resonant electron interwell transitions.

We observed a transition between N- and Z-shaped curves when the number of layers in the structure is varied and studied the corresponding conditions. We found that the structures with sharp transition resonances and low overall conductivity are favorable for the formation of Z-shaped portions of *I-V* curves.

ACKNOWLEDGMENTS

The authors are deeply grateful to Dr. R. V. Belosludov, Dr. A. G. Mironov, Dr. M. A. Ormont, Dr. V. I. Pupyshev, and Professor I. P. Zvyagin for fruitful discussions and comments. The authors would like to express their sincere thanks to the crew of the Center for Computational Materials Science of the Institute for Materials Research, Tohoku University, for their continuous support of the SR8000 supercomputing facilities. This work was supported by Grant No. 1786.2003.2 of the Russian Foundation for Basic Research and a Grant-in-Aid for Scientific Research of the Ministry of Education, Culture, Sports, Science and Technology, Japan.

APPENDIX A

In this work we consider gallium nitride based periodic MQW structures with the following parameters of the material and of the layers: LO-phonon energy $\hbar\omega_{\mathrm{LO}}=92$ meV; effective electron mass $m^*=0.2m_0$; lattice parameter $c=5.17$ Å; dielectric constant $\varepsilon=12.2$; well widths $d_k=12c$ for $k=1,\ldots,N$; barrier widths $b_k=24c$ for $k=2,\ldots,N-2$ and $b_k=12c$ for $k=1,N-1$; well potentials in the absence of the electric field and without charge redistribution in the structure, $u_k^0=0$ for $k=1,\ldots,N$; barrier potentials in the absence of the electric field and without charge redistribution in the structure, $U_k^0=100$ meV for $k=1,\ldots,N-1$; three-dimensional donor concentrations $n_k^0/d_k=10^{15}$ cm^{-3} for $k=2,\ldots,N-1$ and $n_k^0/d_k=10^{19}$ cm^{-3} for $k=1,N$; temperature $T=10$ K. There are two size-quantization levels in each inner quantum well of the structure, with the energies $E_{k,1}=22.8$ meV and $E_{k,2}=81.0$ meV $(k=2,\ldots,N-1)$.

APPENDIX B

The integral probabilities of electron transition between the kth and $(k+1)$th inner quantum wells are defined by the following general expressions:

$$P_k=\sum_{\alpha,\beta}\int W_{k,\alpha;k+1,\beta}(E_k,E_{k,\alpha},E_{k+1},E_{k+1,\beta})\times f_k(E_k)[1-f_{k+1}(E_{k+1})]\frac{2d^2\mathbf{p}_k d^2\mathbf{r}_k}{(2\pi\hbar)^2}\frac{2d^2\mathbf{p}_{k+1}d^2\mathbf{r}_{k+1}}{(2\pi\hbar)^2}\times\left[\sum_{\alpha}\int f_k(E_k)\frac{2d^2\mathbf{p}_k d^2\mathbf{r}_k}{(2\pi\hbar)^2}\right]^{-1}, \tag{B1}$$

$$R_k=\sum_{\alpha,\beta}\int W_{k+1,\beta;k,\alpha}(E_k,E_{k,\alpha},E_{k+1},E_{k+1,\beta})\times f_{k+1}(E_{k+1})[1-f_k(E_k)]\frac{2d^2\mathbf{p}_{k+1}d^2\mathbf{r}_{k+1}}{(2\pi\hbar)^2}\frac{2d^2\mathbf{p}_k d^2\mathbf{r}_k}{(2\pi\hbar)^2}\times\left[\sum_{\alpha}\int f_{k+1}(E_{k+1})\frac{2d^2\mathbf{p}_{k+1}d^2\mathbf{r}_{k+1}}{(2\pi\hbar)^2}\right]^{-1}. \tag{B2}$$

Here $k=2,\ldots,(N-2)$; indices α and β enumerate the size-quantization levels in the kth and $(k+1)$th quantum wells, respectively; $E_{k,\alpha}$ and $E_{k+1,\beta}$ are the energies of these levels; $\mathbf{p}_k$, $\mathbf{r}_k$, $\mathbf{p}_{k+1}$, and $\mathbf{r}_{k+1}$ are the electron in-plane momentum and coordinate vectors in the kth and $(k+1)$th wells; E_k and E_{k+1} are the full energies,

$$E_k=E_{k,\alpha}+\frac{p_k^2}{2m^*},\quad E_{k+1}=E_{k+1,\beta}+\frac{p_{k+1}^2}{2m^*},$$

of the electron states in the kth and $(k+1)$th quantum wells; $W_{k,\alpha;k+1,\beta}$ and $W_{k+1,\beta;k,\alpha}$ are the probabilities per unit time of the direct and reverse transitions between the αth level in the kth well and βth level in the $(k+1)$th well; and f_k and f_{k+1} are the electron distribution functions in the kth and $(k+1)$th quantum wells.

When the barriers are wide enough, the interwell transition time is much greater than the intrawell relaxation time, one can treat f_k as the equilibrium distribution function.

The electron gas can be considered nondegenerate, provided that the electron concentration is much less than the effective density of states in the conduction band.[39] This condition can be fulfilled for relatively low donor concentration in the inner quantum wells, like those mentioned in Appendix A. Then the interwell transition probabilities do not depend upon the electron concentrations, and Fermi factors can be eliminated from formulas (B1) and (B2).

As concerns the contacts, they are usually heavily doped, and the electron concentrations in them may be relatively high; consequently, the Fermi statistics must be used here. The electron energy spectra of the contacts are taken continuous, and the transition from summation to integration in Eqs. (B1) and (B2) gives the probabilities for $k=1$ and $k=N-1$.

All the information concerning the microscopic probability of a particular interwell transition, including energy and in-plane momentum conservation if applicable, is included within $W_{k,\alpha;k+1,\beta}$ and $W_{k+1,\beta;k,\alpha}$. This may lead to a restriction of the integration interval. As an important example, in the present work we consider the probability of interwell transition under assumption that the main electron scattering mechanism is the interaction with ionized impu-

rity. Indeed, at low temperature we can neglect the scattering by acoustical phonons, as well as the absorption of optical phonons. As for the LO-phonon emission, it becomes possible when an electron transition takes place between two levels (either from the same quantum well or from two neighboring wells) with energy difference equal to $\hbar\omega_{\mathrm{LO}}$. However, the distribution function $f_k(E_k)$, which enters Eq. (B1), is non-negligible only when the electron occupies the first size-quantization level of the kth well, with the in-plane kinetic energy $p_k^2/2m^*$ not more than a few meV. For the transitions with such initial energy $[E_k \approx E_{k,1} + (\text{few meV})]$, the optical-phonon scattering can be avoided as long as limited potential drops between the neighboring wells $\Delta u_k < eV_{\max} \approx \hbar\omega_{\mathrm{LO}}$ are considered.[32]

In order to extend the Δu_k limit, we consider material with relatively large LO-phonon energy, namely, gallium nitride (see Appendix A). Importantly, each resonance between the kth and $(k+1)$th wells $(k=1,\ldots,N-1)$ occurs when the potential difference between them is significantly smaller than $\hbar\omega_{\mathrm{LO}}$ of the chosen material (see Fig. 2). However, some Δu_k values, calculated as described in Sec. III for relatively high current densities, may turn out to be still too high. So, the high-voltage regions of the curves in Fig. 3, which correspond to $\Delta u_k > eV_{\max}$ for at least one k, are presented formally. We keep them to provide a better illustration of the phenomenon under study, which is quite general for all the current maxima and independent of the particular Δu_k values. However, one should keep in mind that, strictly speaking, the assumption of the absence of LO-phonon scattering is valid only for the low voltages.

The probability of the interwell transition is proportional to the square of the impurity scattering potential matrix element. On one hand, this matrix element is determined by the overlap of the tails of the wave functions in the neighboring wells. On the other hand, due to the Coulomb scattering involved, it depends on the electron momentum difference between the initial and final states. One can roughly consider these two factors to describe the tunneling and scattering components of the interwell transition, correspondingly. We phenomenologically separate them by the following product:

$$\begin{aligned} W_{k,\alpha;k+1,\beta}(E_k,E_{k,\alpha},E_{k+1},E_{k+1,\beta}) &= W^{(t)}_{k,k+1}(E_{k,\alpha},E_{k+1,\beta}) \\ &\times W^{(s)}_{k,k+1}(E_{k,\alpha},E_{k+1,\beta}) \\ &\times \delta(E_k,E_{k+1}). \end{aligned} \tag{B3}$$

The Kronecker symbol δ equals unity for $E_k = E_{k+1}$, and zero otherwise. It accounts for the total energy conservation, as it is appropriate for the elastic impurity scattering.

The tunneling term $W^{(t)}_{k,k+1}(E)$ in Eq. (B3) can be estimated as the probability current due to the resonant tunneling of an electron with energy E from the kth to the $(k+1)$th quantum well. The probability is proportional to the corresponding transmission coefficient $t_k(E)$:

$$W^{(t)}_{k,k+1}(E_{k,\alpha},E_{k+1,\beta}) = \frac{\sqrt{2(E-u_k)}}{d_k\sqrt{m^*}} t_k(E),$$

where $E = \max(E_{k,\alpha},E_{k+1,\beta})$.

One can estimate $t_k(E)$ as the transmission coefficient through a rectangular potential barrier. Parameters of the barrier are taken such that within the quasiclassical approximation its transparence is equal to that of the kth barrier of the MQW structure. Denoting the height of the rectangular barrier as U and its width as b and using standard quantum mechanics, one finds the following expression for the transmission coefficient:

$$\begin{aligned} t_k(E) = 8(U-E)\sqrt{(E-u_k)(E-u_{k+1})} &\times [\cosh(2\kappa b)(U-u_k)(U-u_{k+1}) \\ &- (U+u_k-2E)(U+u_{k+1}-2E) \\ &+ 4(U-E)\sqrt{(E-u_k)(E-u_{k+1})}]^{-1}, \end{aligned}$$

where $\kappa = \sqrt{2m^*(U-E)}/\hbar$ (compare with the approximate expression in Ref. 3).

As for the dimensionless term $W^{(s)}_{k,k+1}$ in Eq. (B3), in the case of impurity scattering it reaches a maximum when the αth level in the kth well is in resonance with the βth level in the $(k+1)$th well. When a finite level shift $\Delta E = E_{k,\alpha} - E_{k+1,\beta}$ appears, the electron in-plane momentum changes during the elastic transition, and hence the transition matrix element decreases, as described in Sec. II. For simplicity we take the probability dependence on the absolute value of ΔE in the following form:

$$W^{(s)}_{k,k+1}(E_{k,\alpha},E_{k+1,\beta}) = \frac{A^q}{A^q + |\Delta E|^q}.$$

Here the characteristic constant energy A and the dimensionless exponent q are model parameters, and ΔE is the difference between the energies of the electron movement along the growth axis in the initial and final states. The numerical results shown in Figs. 2 and 3 are obtained for the transition probabilities calculated as described here, with $A=1$ meV and $q=1$.

[1] L. Esaki and L. L. Chang, Phys. Rev. Lett. **33**, 495 (1974).
[2] B. Ricco and M. Ya. Azbel, Phys. Rev. B **29**, 1970 (1984).
[3] V. J. Goldman, D. C. Tsui, and J. E. Cunningham, Phys. Rev. Lett. **58**, 1256 (1987).
[4] T. C. L. G. Sollner, Phys. Rev. Lett. **59**, 1622 (1987); V. J. Goldman, D. C. Tsui, and J. E. Cunningham, *ibid.* **59**, 1623 (1987).
[5] V. J. Goldman, D. C. Tsui, and J. E. Cunningham, Phys. Rev. B **35**, R9387 (1987).
[6] F. W. Sheard and G. A. Toombs, Appl. Phys. Lett. **52**, 1228 (1988).
[7] D. D. Coon, K. M. S. V. Bandara, and H. Zhao, Appl. Phys. Lett. **54**, 2115 (1989).
[8] A. D. Martin, M. L. F. Lerch, P. E. Simmonds, and L. Eaves, Appl. Phys. Lett. **64**, 1248 (1994).
[9] M. L. F. Lerch, A. D. Martin, P. E. Simmonds, L. Eaves, and M. L. Leadbeater, Solid-State Electron. **37**, 961 (1994).
[10] V. L. Bonch-Bruevich, I. P. Zvyagin, and A. G. Mironov, *Domain Electrical Instabilities in Semiconductors* (Consultant Bureau, New York, 1975).
[11] A. Wacker and E. Schöll, J. Appl. Phys. **78**, 7352 (1995).
[12] M. N. Feĭginov and V. A. Volkov, JETP Lett. **68**, 662 (1998).
[13] M. Meixner, P. Rodin, E. Schöll, and A. Wacker, Eur. Phys. J. B **13**, 157 (2000).
[14] B. A. Glavin, V. A. Kochelap, and V. V. Mitin, Phys. Rev. B **56**, 13346 (1997).
[15] P. Rodin and E. Schöll, J. Appl. Phys. **93**, 6347 (2003).
[16] A. Wacker, Phys. Rep. **357**, 1 (2002).
[17] L. L. Bonilla, J. Phys.: Condens. Matter **14**, R341 (2002).
[18] L. L. Bonilla, J. Galán, J. A. Cuesta, F. C. Martínez, and J. M. Molera,

Phys. Rev. B **50**, 8644 (1994).
[19]F. Prengel, A. Wacker, and E. Schöll, Phys. Rev. B **50**, 1705 (1994); *ibid.* **52**, 11518 (1995).
[20]A. Wacker, G. Schwarz, F. Prengel, E. Schöll, J. Kastrup, and H. T. Grahn, Phys. Rev. B **52**, 13788 (1995).
[21]G. Schwarz, A. Wacker, F. Prengel, E. Schöll, J. Kastrup, H. T. Grahn, and K. Ploog, Semicond. Sci. Technol. **11**, 475 (1996).
[22]G. Schwarz and E. Schöll, Phys. Status Solidi B **194**, 351 (1996).
[23]G. Schwarz, F. Prengel, E. Schöll, J. Kastrup, H. T. Grahn, and R. Hey, Appl. Phys. Lett. **69**, 626 (1996).
[24]M. Patra, G. Schwarz, and E. Schöll, Phys. Rev. B **57**, 1824 (1998).
[25]A. Wacker, M. Moscoso, M. Kindelan, and L. L. Bonilla, Phys. Rev. B **55**, 2466 (1997).
[26]R. Aguado, G. Platero, M. Moscoso, and L. L. Bonilla, Phys. Rev. B **55**, R16053 (1997).
[27]D. Sánchez, M. Moscoso, L. L. Bonilla, G. Platero, and R. Aguado, Phys. Rev. B **60**, 4489 (1999).
[28]D. Sánchez, M. Moscoso, L. L. Bonilla, G. Platero, and R. Aguado, Physica E (Amsterdam) **7**, 299 (2000).
[29]R. López, D. Sánchez, and G. Platero, Phys. Rev. B **67**, 035330 (2003).
[30]L. L. Bonilla, G. Platero, and D. Sánchez, Phys. Rev. B **62**, 2786 (2000).
[31]A. Amann, A. Wacker, L. L. Bonilla, and E. Schöll, Phys. Rev. E **63**, 066207 (2001).
[32]O. V. Pupysheva and A. V. Dmitriev, Physica E (Amsterdam) **18**, 290 (2003).
[33]While phenomenologically considering the two different parts of the MQW structure, it is important to remember that they are actually inseparable. If isolated, each of these parts would have an electron redistribution, absolutely different from that observed in the total structure. One should keep in mind that the charge distribution is responsible for the feedback mechanism and is thus crucial for the phenomenon discussed here.
[34]M. Tsuchiya and H. Sakaki, Appl. Phys. Lett. **49**, 88 (1986).
[35]E. Schöll, *Nonequilibrium Phase Transitions in Semiconductors* (Springer-Verlag, Berlin, 1987). See detailed discussion of the circuit-induced oscillations in Chap. 6.2.1, pp. 231–239.
[36]B. Jogai and E. T. Koenig, J. Appl. Phys. **69**, 3381 (1991).
[37]A. A. Farajian, K. Esfarjani, and Y. Kawazoe, Phys. Rev. Lett. **82**, 5084 (1999).
[38]F. Léonard and J. Tersoff, Phys. Rev. Lett. **85**, 4767 (2000).
[39]S. M. Sze, *Physics of Semiconductor Devices* (Wiley, New York, 1981).